DMD Fast Forward. Published on April 19, 2006 as doi:10.1124/dmd.105.009126
This article has not been copyedited and formatted. The final version may differ from this version.

NEUROTOXIC PYRIDINIUM METABOLITES OF HALOPERIDOL ARE SUBSTRATES OF HUMAN ORGANIC CATION TRANSPORTERS

Ho-Jin Kang, Sang-Seop Lee, Chung-Hee Lee, Ju-Cheol Shim, Ho Jung Shin, Kwang-Hyeon Liu, Mi-Ae Yoo and Jae-Gook Shin

Department of Pharmacology and PharmacoGenomics Research Center, Inje University College of Medicine, Busan 614-735, Korea (H.J.K., S.S.L., C.H.L., J.C.S., H.J.S., K.H.L., J.G.S.)

Department of Molecular Biology, College of Natural Sciences, Busan National University, Busan 609-735, Korea (H.J.K., M.A.Y.)

TRANSPORT OF NEUROTOXIC METABOLITES OF HALOPERIDOL

Address correspondence to:

Jae-Gook Shin, M.D., Ph.D.

Department of Pharmacology and PharmacoGenomics Research Center

Inje University College of Medicine

Department of Clinical Pharmacology, Busan Paik Hospital

#633-165 Gaegum-Dong, Jin-Gu, Busan 614-735, Korea

Tel: +82-51-890-6709; Fax: +82-51-893-1232

E-mail: phshinjg@inge.ac.kr

Number of text pages: 28

Number of figures: 7

Number of tables: 1

Number of reference: 25

Number of words in abstract: 229

Number of words in introduction: 438

Number of words in discussion: 993

ABBREVIATIONS: hOCTs, human organic cation transporters; HPP^+, 4-(4-chlorophenyl)-1-[4-(4-fluorophenyl)-4-oxybutyl]pyridinium ion; MPP^+, 1-methyl-4-phenylpyridinium**;** $RHPP^+$, 4-(4-(chlorophenyl)-1-4-(fluorophenyl)-4-hydroxybutyl-pyridinium.

DMD Fast Forward. Published on April 19, 2006 as DOI: 10.1124/dmd.105.009126
This article has not been copyedited and formatted. The final version may differ from this version.

Abstract

Two neurotoxic pyridinium metabolites of haloperidol, HPP^+ and $RHPP^+$, are formed in the liver and found in the brain. To understand how these neurotoxic pyridinium metabolites are distributed in the brain, HPP^+ and $RHPP^+$ were evaluated as substrates for human organic cation transporters (hOCTs). Both HPP^+ and $RHPP^+$ were accumulated in Caco-2 cells, and these accumulations were significantly inhibited by pretreatment with the hOCT inhibitors verapamil, cimetidine, phenoxybenzamine, and corticosterone. The contribution of each hOCT was evaluated based on measurements of the intracellular concentrations of haloperidol metabolites in MDCK cells transfected with hOCT1, hOCT2, or hOCT3. HPP^+ accumulated in hOCT-overexpressing MDCK cells in a concentration-dependent manner, with estimated K*m* values of 0.99, 2.79, and 2.23 μM, and V*max* values of 282.1, 256.1, and 400.2 pmol/min/μg protein for hOCT1, hOCT2, and hOCT3, respectively. $RHPP^+$ accumulated in hOCT1- and hOCT3-overexpressing MDCK cells, with estimated K*m* values of 5.15 and 8.21 μM and V*max* values of 1230.9 and 1348.6 pmol/min/μg protein for hOCT1 and hOCT3, respectively. On the other hand, $RHPP^+$ did not accumulate in the hOCT2-expressing MDCK cells. These results suggest that HPP^+ and $RHPP^+$ are substrates for hOCTs, with the exception of $RHPP^+$ for hOCT2. Thus, hOCTs appear to contribute to the disposition of these toxic metabolites in human subjects, although further *in vivo* studies are required to elucidate the involvement of hOCTs in the disposition of haloperidol pyridinium metabolites.

DMD Fast Forward. Published on April 19, 2006 as DOI: 10.1124/dmd.105.009126
This article has not been copyedited and formatted. The final version may differ from this version.

Introduction

The antipsychotic drug haloperidol is biotransformed into several metabolites, including reduced haloperidol and a number of pyridinium metabolites, such as HPP^+ {4-(4-chlorophenyl)-1-[4-(4-fluorophenyl)-4-oxybutyl]pyridinium ion} and $RHPP^+$ (a reduced form of HPP^+), in humans (Eyles et al., 1994; Igarashi et al., 1995). Haloperidol pyridinium metabolites are structurally similar to the neurotoxin MPP^+ (1-methyl-4-phenylpyridinium; Fig. 1), which is known to cause neurodegeneration, and have been reported as having similar or more potent neurotoxic effects, e.g., inhibition of mitochondrial respiration, irreversible inhibition of tyrosine hydroxylase, and depletion of dopamine and serotonin (Bloomquist et al., 1994; Rollema et al., 1994; Fang et al., 1995). The formation of toxic pyridinium metabolites of haloperidol is mediated primarily by hepatic cytochrome P450 3A (Igarashi et al., 1995), although it has not been clearly established how the cationic metabolite HPP^+ formed in peripheral tissues becomes localized to the brain (Igarashi and Castagnoli, 1992; Igarashi, 1998).

HPP^+ has been detected in the brains of patients who have chronically received haloperidol (Bloomquist et al., 1994). Furthermore, HPP^+ shows a moderate brain uptake index, which indicates that it may permeate the blood-brain barrier. These results support the hypothesis that HPP^+ is formed mainly in the liver, circulates in the bloodstream, and enters the brain, where it induces damage to brain dopaminergic neurons (Kawashima et al., 2002; Kawashima et al., 2004).

Recent reports have suggested that MPP^+ is a high-affinity substrate for the human organic cation transporters hOCT1, hOCT2, and hOCT3 (Hayer-Zillgen et al., 2002). The

hOCT1 and hOCT2 forms are expressed predominantly in the liver and kidneys, respectively (Gorboulev et al., 1997), whereas hOCT3 (also known as extraneuronal monoamine transporter or EMT), which also has a high affinity for monoamines, is highly expressed in the placenta (Verhaagh et al., 1999). Recently, it has been reported that hOCT3 may play a significant role in the disposition of cationic neurotoxins and neurotransmitters in the brain (Wu et al., 1998). Since MPP^+ is metabolically stable as a charged molecule and shows low-level diffusion across the cytoplasmic membrane, it accumulates exclusively in nerve cells, in a distribution process that may be mediated by hOCTs (Russ et al., 1992). Although HPP^+ is less potent than MPP^+ in the dopaminergic system, these compounds display comparable toxic effects on the serotonergic system. Considering the structural similarities between MPP^+ and both haloperidol metabolites, it seems likely that these metabolites represent substrates for hOCTs.

In the present study, we evaluate whether the toxic haloperidol pyridinium metabolites HPP^+ and $RHPP^+$ are substrates for hOCTs. In addition, we characterize HPP^+ and $RHPP^+$ uptake into hOCT-overexpressing MDCK cells, to clarify the potential contribution of hOCTs to the disposition of these two metabolites.

DMD Fast Forward. Published on April 19, 2006 as DOI: 10.1124/dmd.105.009126
This article has not been copyedited and formatted. The final version may differ from this version.

Materials and Methods

Chemicals and Reagents.

Verapamil, cimetidine, phenoxybenzamine, and corticosterone were purchased from Sigma Chemical Co. (St Louis, MO). The 4-(4-chlorophenyl)-1-[4-(4-fluorophenyl)-4-oxobutyl]pyridinium (HPP^+) and 4-(4-(chlorophenyl)-1-4-(fluorophenyl)-4-hydroxybutyl-pyridinium ($RHPP^+$) were generous gifts from Dr. Neal Castagnoli, Jr. (Department of Chemistry, Virginia Polytechnic Institute and State University, Blacksburg, VA). N-[methyl-^{3}H]-methyl-4-phenylpyridinium acetate (MPP^+) (3.21 TBq/mmol) and tetraethylammonium bromide, [1-14C]-, TEA (185 MBq/mmol) were purchased from PerkinElmer (Boston, MA). Dulbecco's modified Eagle's medium (DMEM), fetal bovine serum (FBS), trypsin, and Lipofectamine^{TM} 2000 were purchased from Gibco-BRL (Invitrogen, Carlsbad, CA).

Cell Culture and Stable Transfection of hOCT1, hOCT2 and hOCT3.

Caco-2 cells were maintained in a humidified atmosphere of 5% CO_2 in air and were grown in DMEM that was supplemented with 20% FBS, 2 mM L-glutamine, 1% non-essential amino acids, and 100 U/ml penicillin-streptomycin. The medium was changed every second day. For the uptake assay, 5×10^5 Caco-2 cells were seeded on 12-well plastic cell culture clusters. The uptake studies were usually performed 7 to 9 days after the cells formed a monolayer. MDCK cells were maintained in a humidified atmosphere of 5% CO_2 in air and were grown in DMEM that was supplemented with 10% FBS, 2 mM L-glutamine, and 100 U/ml penicillin-streptomycin. For the construction of stable hOCT1-, hOCT2-, and

DMD Fast Forward. Published on April 19, 2006 as DOI: 10.1124/dmd.105.009126
This article has not been copyedited and formatted. The final version may differ from this version.

hOCT3-expressing cells, the MDCK cells were transfected with pcDNA3.1 plasmids that carried the genes for hOCT1, hOCT2, and hOCT3, respectively, using Lipofectamine 2000. The stable cells were selected for resistance to 800 mg/ml geneticin (G418; Life Technologies, Karlsruhe, Germany) for 3 weeks (Hayer-Zillgen et. al., 2002). The expression levels of hOCT1, hOCT2, and hOCT3 were verified in functional assays and Western blots. For the uptake assay, 5×10^5 cells were seeded on 12-well plastic cell culture clusters. The uptake assay was performed after monolayer formation.

Plasmids.

The plasmids pEXO-hOCT1 and pEXO-hOCT2, which contain the hOCT1 and hOCT2 cDNAs, respectively, were kindly provided by Dr. Kathleen M. Giacomini (University of California, San Francisco, CA). The hOCT1- and hOCT2-coding regions were amplified from these plasmids using PCR and Pfu DNA polymerase. The following specific primers were designed based on the nucleotide sequences for human OCT1 and OCT2 (GenBank accession no. NM_003057 and NM_003058): hOCT1 forward, 5′-GCCGGTACCATGCCCACCGTGGATGACATTC-3′ and reverse, 5′-GCCGGTACCTCAGGTGCCCGAGGGTTCTG-3′; and hOCT2 forward, 5′-GCCGGTACCATGCCCACCACCGTGGAC-3′ and reverse, 5′-GCCGGTACCTTAGTTCAATGGAATGTCTAGTTTCTG-3′ (*Kpn*I restriction sites underlined). The isolated cDNAs were subcloned into the *Kpn*I site of pcDNA3.1(-) (Invitrogen, The Netherlands). The plasmid pcDNA 3.1(+)-hOCT3 (NM_021977) was kindly provided by Dr. Hitoshi Endou (Fuji Biomedix Co., Ltd., Tokyo, Japan).

DMD Fast Forward. Published on April 19, 2006 as DOI: 10.1124/dmd.105.009126
This article has not been copyedited and formatted. The final version may differ from this version.

Cellular Accumulation Assay.

Before the cellular accumulation assay, the growth medium was removed from the cell cultures and the attached cells were washed with Eagle's medium and pre-incubated in serum-free DMEM at 37°C for 1 h. The uptake study was initiated by the addition of 1 ml of medium that contained 200 nM [^{3}H]MPP$^+$ or [^{14}C]TEA and 10 μM HPP$^+$ or RHPP$^+$, in the absence or presence of known hOCT inhibitors i.e., 100 μM verapamil, 50 μM phenoxybenzamine, 50 μM cimetidine, or 50 μM corticosterone at 37°C. The uptake study was stopped by three washes with 2 ml of ice-cold phosphate-buffered saline, and the cells were lysed with 100 μl of 1× cell culture lysis reagent (CCLR buffer; Promega, Madison, WI), which contained 100 mM potassium phosphate (pH 7.8), 1 mM EDTA, 7 mM 2-mercaptoethanol, 1% (v/v) Triton X-100, and 10% (v/v) glycerol. The levels of [^{3}H]MPP$^+$ and [^{14}C]TEA radioactivity in the cell lysates were measured using the MicroBeta TriLux 96-well Scintillation/Luminescence Detector (Wallac Oy, Turku, Finland). For the measurement of HPP$^+$ and RHPP$^+$, the cells were lysed by the addition of 200 μl acetonitrile/citrate buffer (90:10) (Zhang et al., 2002) and incubation at room temperature for 10 min, followed by shaking for 10 min. The cell lysates were transferred to microcentrifuge tubes on ice, and the supernatant was recovered after centrifugation at 13,000 rpm for 3 min. The concentrations of HPP$^+$ and RHPP$^+$ were determined by liquid chromatography-tandem mass spectrometry (LC/MS/MS).

Measurements of HPP$^+$ and RHPP$^+$ Using LC/MS/MS.

The HPP$^+$ and RHPP$^+$ standards were dissolved in methanol at a concentration of 10 μM. These stock solutions were serially diluted with methanol to concentrations of 0.1,

0.5, 1, 5, 10, 20, 50, and 100 nM. The concentrations of HPP^+ and $RHPP^+$ in acetonitrile/citrate were quantified using liquid chromatography mass spectrometry with the PE SCIEX API 3000 LC/MS/MS system (Applied Biosystems, Foster City, CA), which was equipped with an electrospray ionization interface that was used to generate positive ions $[M^+H]^+$. The compounds were separated on a reversed-phase column (Luna C18, 5 mm × 50 mm internal diameter, 3-μm particle size; Phenomenex, Torrance, CA) with an isocratic mobile phase that consisted of acetonitrile and 5 mM ammonium acetate buffer (70:30). The mobile phase was eluted at 0.2 ml/min using an HP 1100 series pump (Agilent, Wilmington, DE). The turboion spray interface was operated in the positive ion mode at 5500 V and 350°C. The operating conditions, which were optimized by the flow injection of a mixture of all the analytes, were as follows: nebulizing gas flow, 1.04 L/min; auxiliary gas flow, 4.0 L/min; curtain gas flow, 1.44 L/min; orifice voltage, 80 V; ring voltage, 400 V; and collision gas (nitrogen) pressure, 3.58×10^{-5} Torr. The quantitation was performed by multiple reaction monitoring (MRM) of the protonated precursor ion and the related product ion for HPP^+ and $RHPP^+$, using the internal standard method with peak area ratios and a weighting factor of $1/x$. The mass transitions used for HPP^+ and $RHPP^+$ were m/z 354→165 and 356→149, respectively (collision energy, 40 eV; dwell time, 200 ms). Quadrupoles Q1 and Q3 were set on unit resolution. The analytical data were processed using the Analyst software ver. 1.2 (Applied Biosystems). Most of the cell lysates were analyzed directly without dilution. One microliter of each lysate was injected into the column. For the first minute of each run, the elution was diverted to waste. The HPP^+ and $RHPP^+$ concentrations in the lysates were within the standard curve range.

DMD Fast Forward. Published on April 19, 2006 as DOI: 10.1124/dmd.105.009126
This article has not been copyedited and formatted. The final version may differ from this version.

Western Blotting.

Since the uptake of HPP^+ and $RHPP^+$ is influenced by the expression levels of hOCTs in the membrane, the intracellular concentrations of both metabolites were adjusted according to the hOCT expression levels. The levels of expressed hOCTs were determined by Western blotting. For the total protein extracts, transiently transfected or stably expressed cells of MDCK-hOCT1, MDCK-hOCT2, and MDCK-hOCT3 were lysed with one volume of RIPA cell lysis buffer [150 mM NaCl, 1% NP-40, 0.5% sodium deoxycholate, 0.1% SDS, 50 mM Tris-Cl (pH 7.5)] for 10 min. The samples were separated by SDS-polyacrylamide 4-12% gradient gel electrophoresis, and then electroblotted onto nitrocellulose membranes (Bio-Rad, Hercules, CA). The nitrocellulose membranes were incubated with 5% non-fat dry milk in TBST for 2 h. The membranes were then incubated with polyclonal antibodies against OCT1, OCT2, and OCT3 (Santa Cruz Biotechnology, Santa Cruz, CA) and an anti-actin antibody (Cell Signaling Technology, Beverly, MA) overnight at 4°C. After rinsing with TEST, the membranes were incubated with HRP-labeled anti-goat IgG antibody or anti-rabbit IgG antibody (Santa Cruz Biotechnology) and visualized using the Enhanced ChemiLuminescence (ECL) System (Santa Cruz Biotechnology).

Data Analysis.

Uptake was calculated as the cell:medium ratio based on the intracellular uptake per microgram of cell protein per min (dpm/min/μg protein or MRM/min/μg protein) relative to the initial drug concentration. The K_m and V_{max} values for substrate uptake were

DMD Fast Forward. Published on April 19, 2006 as DOI: 10.1124/dmd.105.009126

estimated by nonlinear least-squares regression analysis to the Michaelis-Menten equation using the WinNonlin software (Pharsight, Mountain View, CA). Transporter-mediated HPP^+ or $RHPP^+$ uptake was calculated by subtracting the uptake levels in mock cells from the net uptake in transfected cells for the kinetic study. Statistical significance was analyzed using the Student's *t*-test, and $p < 0.05$ was considered to be statistically significant. The reproducibility of the results in the present study was confirmed by two or three subsequent experiments, and all the data are expressed as the mean ± S.E.M. of three replicates.

DMD Fast Forward. Published on April 19, 2006 as DOI: 10.1124/dmd.105.009126
This article has not been copyedited and formatted. The final version may differ from this version.

Results

Intracellular Accumulations of HPP^+ and $RHPP^+$ in Caco-2 Cells.

Since Caco-2 cells express several drug transporters, including hOCT1 and hOCT3 (Matel et al., 2001), hOCT-mediated cellular uptake of [^{3}H]MPP^+, which is a well-known hOCT substrate, was determined in Caco-2 cells, as a positive control. Caco-2 cells were incubated with 200 nM [^{3}H]MPP^+ for various periods of time in the absence or presence of 100 μM verapamil, a known hOCT inhibitor. The cellular uptake of [^{3}H]MPP^+ increased non-linearly for up to 90 min (Fig. 2A). In the presence of verapamil, the intracellular concentration of [^{3}H]MPP^+ in Caco-2 cells was significantly reduced, by two-fold, within 90 min (Fig. 2A). When the haloperidol metabolites 10 μM HPP^+ and $RHPP^+$ were incubated under the same conditions as for [^{3}H]MPP^+, the intracellular concentrations of HPP^+ and $RHPP^+$ showed no proportional increases, although saturation was not complete until the cells were incubated for 90 min (Fig. 2B and 2C). However, the intracellular accumulations of HPP^+ and $RHPP^+$ in Caco-2 cells were significantly reduced by about two-fold in the presence of verapamil for 90 min (Fig. 2B and 2C). The intracellular concentrations of HPP^+ and $RHPP^+$ were also significantly reduced by the addition of other inhibitors of OCT1, OCT2, and OCT3, i.e., phenoxybenzamine, cimetidine, and corticosterone (Fig. 3).

Intracellular Accumulations of HPP^+ and $RHPP^+$ in hOCT1-, hOCT2-, and hOCT3-expressing MDCK Cells.

To further characterize hOCT-mediated uptake of HPP^+ and $RHPP^+$, the

DMD Fast Forward. Published on April 19, 2006 as DOI: 10.1124/dmd.105.009126
This article has not been copyedited and formatted. The final version may differ from this version.

intracellular concentrations of these metabolites were evaluated in MDCK cells that transiently overexpressed hOCT1, hOCT2, and hOCT3. Twenty-four hours after transfection of the MDCK cells with each of the hOCTs, 200 nM [^{3}H]MPP$^+$, 10 μM HPP$^+$ or 10 μM RHPP$^+$ were added for 30 min at 37°C in the absence or presence of 50 μM phenoxybenzamine (Fig. 4). The activities of the overexpressed hOCTs were confirmed by the two- to three-fold higher [^{3}H]MPP$^+$ uptake into the hOCT1-, hOCT2-, and hOCT3-overexpressing cells, as compared to vector-transfected, control, mock-treated cells (Fig. 4A). The level of [^{3}H]MPP$^+$ uptake was significantly reduced in the presence of phenoxybenzamine in the hOCT-transfected MDCK cells, as well as in the mock-treated cells. The uptake of HPP$^+$ was also increased by two- to three-fold in MDCK cells that overexpressed hOCT1, hOCT2, and hOCT3 (Fig. 4B), whereas RHPP$^+$ uptake was not increased in MDCK cells that overexpressed hOCT2 (Fig. 4C). Furthermore, overexpression of the hOCT1, hOCT2, and hOCT3 proteins was verified by Western blotting (Fig. 4D). For the kinetic analysis of HPP$^+$ and RHPP$^+$ uptake, we established MDCK cells that stably expressed hOCT1, hOCT2, and hOCT3, and measured the uptake of HPP$^+$ and RHPP$^+$ by these cells. The functional expression of hOCT1, hOCT2, and hOCT3 was verified by [^{3}H]MPP$^+$ and [^{14}C]TEA uptake assays (Fig. 5A, B) and by Western blotting (Fig. 5C). The kinetics of HPP$^+$ and RHPP$^+$ uptake were examined by incubating the MDCK cells that stably expressed hOCTs with either 10 μM HPP$^+$ or 10 μM RHPP$^+$ at 37°C for various periods of time (1, 5, 10, 15, 30, 60 or 90 min) (Fig. 6A, B). The rates of uptake of HPP$^+$ and RHPP$^+$ were nonlinear for up to 90 min in the MDCK cells that overexpressed hOCT1, hOCT2, and hOCT3. However, RHPP$^+$ was not transported by hOCT2-overexpressing MDCK cells.

DMD Fast Forward. Published on April 19, 2006 as DOI: 10.1124/dmd.105.009126
This article has not been copyedited and formatted. The final version may differ from this version.

The concentration dependencies of the uptake rates were studied by incubating hOCT1-, hOCT2-, and hOCT3-expressing MDCK cells with increasing concentrations (0, 0.1, 0.5, 1, 2, 3, 5, 10, and 15 μM) of HPP^+ or $RHPP^+$ for 15 min at 37°C (Fig. 7). From the uptake study, HPP^+ accumulated in hOCT-overexpressing MDCK cells in a concentration-dependent manner, with estimated K*m* values of 0.99, 2.79, and 2.23 μM, and V*max* values of 282.1, 256.1, and 400.2 pmol/min/μg protein for hOCT1, hOCT2, and hOCT3, respectively (Fig. 7A, B and C) (Table 1). $RHPP^+$ accumulated in the hOCT1- and hOCT3-overexpressing MDCK cells, with estimated K*m* values of 5.15 and 8.21 μM, and V*max* values of 1230.9 and 1348.6 pmol/min/μg protein for hOCT1 and hOCT3, respectively (Fig. 7D, E) (Table 1). These results suggest that both HPP^+ and $RHPP^+$ are substrates for hOCTs, with the exception of $RHPP^+$ for hOCT2.

DMD Fast Forward. Published on April 19, 2006 as DOI: 10.1124/dmd.105.009126
This article has not been copyedited and formatted. The final version may differ from this version.

Discussion

Chronic use of the antipsychotic drug haloperidol causes adverse neurodegenerative events in patients. This toxicity has been attributed to the distribution of the toxic haloperidol metabolites HPP^+ and $RHPP^+$ into the brain, with consequent neuronal cell death. Haloperidol can be biotransformed into toxic metabolites by the action of cytochrome P450 3A4 (CYP3A4), which is a major hepatic drug-metabolizing enzyme. Since CYP3A4 expression is rare or limited in the brain, it has been postulated that haloperidol metabolites are formed in peripheral tissues and subsequently transported into the brain. However, to date there have been no reports of transporters for haloperidol metabolites, which might lend support to the notion of unique distribution patterns for these neurotoxic cationic compounds.

In the present study, we identified the transporters for HPP^+ and $RHPP^+$ as hOCTs. Haloperidol metabolites are structurally similar to the neurotoxin MPP^+ (Fig. 1), which is an agent of neurodegeneration. Structurally, these compounds share a highly cationic pyridinium group. Functionally, they exhibit similar brain toxicities in terms of neuronal cell death, attributable to the inhibition of mitochondrial function. Initially, we investigated the transport of haloperidol metabolites into Caco-2 cells, which express various kinds of transporters and are able to transport organic cations across membranes *via* two distinct Na^+-independent transporters, hOCT1 and hOCT3 (Martel et al., 2001). Caco-2 cells represent an appropriate model system for intestinal epithelial permeability studies, and the Caco-2 cell system offers considerable advantages for the study of the functional properties of transport processes, as compared to the use of intestinal tissues *in vivo* or *in vitro* (Matel

et al., 2000). MPP^+, which is a cationic compound, has also been identified as a substrate for hOCTs. Considering the similarities between MPP^+ and haloperidol metabolites, we hypothesized that hOCTs mediate the transport of haloperidol metabolites. Therefore, we investigated the levels of accumulation of HPP^+ and $RHPP^+$ in Caco-2 cells and inhibited these transport processes using hOCT inhibitors.

The intracellular uptake of HPP^+ and $RHPP^+$ in Caco-2 cells showed nonlinear saturation (Fig. 2B, C). Pretreatment with hOCT inhibitors, such as verapamil (Matel et al., 2000), cimetidine (Zang et al., 1997; Grundemann et al., 1998), phenoxybenzamine, and corticosterone (Hayer-Zillgen et al., 2002), significantly reduced haloperidol metabolite uptake (Figs. 2 and 3). These compounds markedly inhibited hOCT function, although their effects on other transporters have not been fully investigated. Furthermore, phenoxybenzamine is a very specific inhibitor of hOCTs and has no known inhibitory effects on other transporters. Therefore, the inhibition of haloperidol metabolite uptake by these hOCT inhibitors suggests that hOCTs mediate the transport of these drugs.

The role of hOCTs in haloperidol metabolite uptake was demonstrated in MDCK cells that overexpressed hOCT1, hOCT2, or hOCT3. Cells that overexpressed hOCT1 and hOCT3 accumulated HPP^+ and $RHPP^+$, and the specificity of transport was verified by pretreatment with hOCT inhibitor (Fig. 4). HPP^+ was accumulated to high levels in MDCK cells that stably expressed the hOCTs (Fig. 6). Interestingly, hOCT2-expressing cells accumulated HPP^+ but not $RHPP^+$. These results indicate that each hOCT has a different substrate spectrum.

Human organic cation transporter systems have been studied primarily in the kidney and liver because these organs play major roles in the elimination of xenobiotics

(Pritchard and Miller, 1993; Ullrich, 1994). The hOCT1 and hOCT2 isoforms are primarily expressed in the liver and kidney, respectively, and to a lesser degree in the small intestine (Gorboulev et al., 1997; Busch et al., 1998; Zhang et al., 1998). These two hOCTs exhibit considerable overlap in terms of substrate specificity, as revealed by MPP^+ and HPP^+. The neuronal toxicity of haloperidol results from the toxic products of its metabolism, which is mediated mainly by CYP3A4 and partially by another P450 isoform, CYP2D6. CYP3A4 is highly expressed in the liver and intestine. Thus, haloperidol can be metabolized by CYP3A4 in hepatocytes and intestinal epithelia and then transported into the bile duct and bloodstream through the actions of hOCT1 and hOCT2. The metabolites can be eliminated in the urine through hOCTs, which are highly expressed in the kidney. The contributions of hOCT1 and hOCT2 to the hepatic, intestinal, and renal transport of haloperidol metabolites need to be studied further *in vivo*, to develop a better understanding of haloperidol disposition.

Several cationic neurotoxins and neurotransmitters are good substrates for hOCT1 and hOCT2 (Pritchard and Miller, 1993; Ullrich, 1994) and, given the potential roles of these transporters in the handling of neurotoxins and neurotransmitters, attempts have been made to detect the expression of hOCT1 and hOCT2 in the brain (Grundemann et al., 1994; Gorboulev et al., 1997; Zhang et al., 1998). Although hOCT1 and hOCT2 mRNAs were not detected in the brain by Northern blot analysis (Gorboulev et al., 1997; Zhang et al., 1997), the results of studies using more sensitive RT-PCR methods have indicated that hOCT2-specific transcripts are present in the brain (Gorboulev et al., 1997; Grundemann et al., 1997). The neuronal expression of hOCT2 has been suggested by *in situ* hybridization and immunocytochemistry results (Busch et al., 1998). Assuming that hOCT2 is expressed in

the blood-brain barrier, even at a low level, it may contribute to the distribution of haloperidol into the brain. Given that hOCT2 has been shown to transport HPP^+ in an effective manner in the present study, the HPP^+ formed in peripheral tissues may be taken up into the brain by the hOCT2 transporter.

Another hOCT isoform, hOCT3, was first identified as the corticosterone-sensitive extraneuronal catecholamine transporter, and has been detected in the brain cortex as well as in liver and heart tissues (Grundemann et al., 1998). The ability of hOCT3 to interact with cationic neurotoxins and neurotransmitters, and the expression of hOCT3 in the brain, suggest that hOCT3 plays a role in the distribution of haloperidol metabolites into the brain. Considering that hOCT3 is an effective transporter of HPP^+ and $RHPP^+$, it is possible that hOCT3 contributes to the transport of these neurotoxic metabolites. Further *in vivo* studies are required to investigate whether hOCT3 mediates the distribution of haloperidol pyridinium metabolites into the brain.

DMD Fast Forward. Published on April 19, 2006 as DOI: 10.1124/dmd.105.009126
This article has not been copyedited and formatted. The final version may differ from this version.

Acknowledgements

The authors thank Dr. Neal Castagnoli, Jr. for providing HPP^+ and $RHPP^+$. The hOCT-containing plasmids were kindly provided by Dr. Kathleen M. Giacomini and Dr. Hitoshi Endou.

DMD Fast Forward. Published on April 19, 2006 as DOI: 10.1124/dmd.105.009126
This article has not been copyedited and formatted. The final version may differ from this version.

References

Bloomquist J, King E, Wright A, Mytilineou C, Kimura K, Castagnoli K, and Castagnoli N, Jr. (1994) 1-Methyl-4-phenylpyridinium-like neurotoxicity of a pyridinium metabolite derived from haloperidol: cell culture and neurotransmitter uptake studies. *J Pharmacol Exp Ther* **270**:822–830.

Busch AE, Karbach U, Miska D, Gorboulev V, Akhoundova A, Volk C, Arndt P, Ulzheimer JC, Sonders MS, Baumann C, Waldegger S, Lang F, and Koepsell H (1998) Human neurons express the polyspecific cation transporter hOCT2, which translocates monoamine neurotransmitters, amantadine, and memantine. *Mol Pharmacol* **54**:342–352.

Eyles DW, McLennan HR, Jones A, McGrath JJ, Stedman TJ, and Pond SM (1994) Quantitative analysis of two pyridinium metabolites of haloperidol in patients with schizophrenia. *Clin Pharmacol Ther* **56**:512–520.

Fang J, Zuo D, and Yu PH (1995) Comparison of cytotoxicity of a quaternary pyridinium metabolite of haloperidol (HPP+) with neurotoxin N-methyl-4-phenylpyridinium (MPP+) towards cultured dopaminergic neuroblastoma cells. *Psychopharmacology (Berl)* **121**:373–378.

Gorboulev V, Ulzheimer JC, Akhoundova A, Ulzheimer-Teuber I, Karbach U, Quester S, Baumann C, Lang F, Busch AE, and Koepsell H (1997) Cloning and characterization of two human polyspecific organic cation transporters. *DNA Cell Biol* **16**:871–881.

Grundemann D, Babin-Ebell J, Martel F, Ording N, Schmidt A, and Schomig E (1997) Primary structure and functional expression of the apical organic cation transporter from kidney epithelial LLC-PK1 cells. *J Biol Chem* **272**:10408–10413.

Grundemann D, Gorboulev V, Gambaryan S, Veyhl M, and Koepsell H (1994) Drug excretion mediated by a new prototype of polyspecific transporter. *Nature* **372**:549–552.

Grundemann D, Schechinger B, Rappold GA, and Schomig E (1998) Molecular identification of the corticosterone-sensitive extraneuronal catecholamine transporter. *Nat Neurosci* **1**:349–351.

Hayer-Zillgen M, Bruss M, and Bonisch H (2002) Expression and pharmacological profile of the human organic cation transporters hOCT1, hOCT2 and hOCT3. *Br J Pharmacol* **136**:829–836.

Igarashi K (1998) The possible role of an active metabolite derived from the neuroleptic agent haloperidol in drug-induced Parkinsonism. *Journal of Toxicology - Toxin Reviews* **17**:27–38.

Igarashi K and Castagnoli N, Jr. (1992) Determination of the pyridinium metabolite derived from haloperidol in brain tissue, plasma and urine by high-performance liquid chromatography with fluorescence detection. *J Chromatogr* **579**:277–283.

Igarashi K, Kasuya F, Fukui M, Usuki E, and Castagnoli N, Jr. (1995) Studies on the metabolism of haloperidol (HP): the role of CYP3A in the production of the neurotoxic pyridinium metabolite HPP+ found in rat brain following ip administration of HP. *Life Sci* **57**:2439–2446.

Kawashima H, Iida Y, Kitamura Y, Kiyono Y, Magata Y, and Saji H (2002) Brain extraction of 4-(4-chlorophenyl)-1-[4-(4-fluorophenyl)-4-oxobutyl]pyridinium ion (HPP+), a neurotoxic metabolite of haloperidol: studies using [3H]HPP+. *Jpn J Pharmacol* **89**:426–428.

Kawashima H, Iida Y, Kitamura Y, and Saji H (2004) Binding of 4-(4-chlorophenyl)-1-[4-

(4-fluorophenyl)-4-oxobutyl]pyridinium ion (HPP+), a metabolite of haloperidol, to synthetic melanin: implications for the dopaminergic neurotoxicity of HPP+. *Neurotox Res* **6**:535–542.

Martel F, Calhau C, and Azevedo I (2000) Characterization of the transport of the organic cation [^{3}H]MPP+ in human intestinal epithelial (Caco-2) cells *Naunyn Schmiedebergs Arch Pharmacol* **361**:505–513

Martel F, Grundemann D, Calhau C, and Schomig E (2001) Apical uptake of organic cations by human intestinal Caco-2 cells: putative involvement of ASF transporters. *Naunyn Schmiedebergs Arch Pharmacol* **363**:40–49.

Pritchard JB and Miller DS (1993) Mechanisms mediating renal secretion of organic anions and cations. *Physiol Rev* **73**:765–796.

Rollema H, Skolnik M, D'Engelbronner J, Igarashi K, Usuki E, and Castagnoli N, Jr. (1994) MPP(+)-like neurotoxicity of a pyridinium metabolite derived from haloperidol: in vivo microdialysis and in vitro mitochondrial studies. *J Pharmacol Exp Ther* **268**:380–387.

Russ H, Gliese M, Sonna J, and Schomig E (1992) The extraneuronal transport mechanism for noradrenaline (uptake2) avidly transports 1-methyl-4-phenylpyridinium (MPP+). *Naunyn Schmiedebergs Arch Pharmacol* **346**:158–165.

Ullrich KJ (1994) Specificity of transporters for 'organic anions' and 'organic cations' in the kidney. *Biochim Biophys Acta* **1197**:45–62.

Verhaagh S, Schweifer N, Barlow DP, and Zwart R (1999) Cloning of the mouse and human solute carrier 22a3 (Slc22a3/SLC22A3) identifies a conserved cluster of three organic cation transporters on mouse chromosome 17 and human 6q26-q27. *Genomics* **55**:209–218.

Wu X, Kekuda R, Huang W, Fei YJ, Leibach FH, Chen J, Conway SJ, and Ganapathy V (1998) Identity of the organic cation transporter OCT3 as the extraneuronal monoamine transporter (uptake2) and evidence for the expression of the transporter in the brain. *J Biol Chem* **273**:32776–32786.

Zhang L, Brett CM, and Giacomini KM (1998) Role of organic cation transporters in drug absorption and elimination. *Annu Rev Pharmacol Toxicol* **38**:431–460.

Zhang L, Dresser MJ, Gray AT, Yost SC, Terashita S, and Giacomini KM (1997) Cloning and functional expression of a human liver organic cation transporter. *Mol Pharmacol* **51**:913–921.

Zhang Q, Pang WL, Chen H, Cherrington J, Lipson K, Antonian L, and Shawver LK (2002) Application of LC/MS/MS in the quantitation of SU101 and SU0020 uptake by 3T3/PDGFr cells. *J Pharm Biomed Anal* **28**:701–709.

Footnotes

Financial supports;

This work was supported by grants from the Ministry of Health & Welfare, Republic of Korea (02-PJ2-PG6-DC04-0001) and the Ministry of Science and Technology (National Research Laboratory Program).

DMD Fast Forward. Published on April 19, 2006 as DOI: 10.1124/dmd.105.009126
This article has not been copyedited and formatted. The final version may differ from this version.

Legends for Figures

FIG. 1. MPP^+-like neurotoxic pyridinium metabolites of haloperidol, HPP^+ and $RHPP^+$.

FIG. 2. Time-course analyses of [^{3}H]MPP^+, HPP^+, and $RHPP^+$ accumulations in Caco-2 cells. A. [^{3}H]MPP^+ (200 nM) was applied to the apical side of the Caco-2 cell monolayer and incubated for 0, 5, 10, 15, 30, 60, or 90 min at 37°C in the absence or presence of 100 μM verapamil. **B and C.** HPP^+ (10 μM) or $RHPP^+$ (10 μM) was applied to the apical side of the Caco-2 cell monolayer and incubated for 0, 5, 10, 15, 30, 60, or 90 min at 37°C in the absence or presence of 100 μM verapamil. The cellular concentrations of HPP^+ and $RHPP^+$ were determined by LC/MS/MS analysis. Exponential saturation curves were fitted to the experimental data. Linear coefficient (r^2) = 0.9990. The data are presented as arithmetic mean ± SEM (n = 3). ** $p < 0.01$.

FIG. 3. Effect of organic cation transporter inhibitors on HPP^+ and $RHPP^+$ accumulations in human intestinal Caco-2 cells. Cells were incubated for 30 min at 37°C with 10 μM HPP^+ or 10 μM $RHPP^+$, which was applied to the apical cell border, in the absence or presence of 50 μM phenoxybenzamine (Phe), 50 μM cimetidine (Cim) or 50 μM corticosterone (Cot), which are known to inhibit hOCT activities *in vitro*. The cellular concentrations of HPP^+ and $RHPP^+$ were determined by LC/MS/MS analysis. The data are presented as arithmetic mean ± SEM (n = 3). ** $p < 0.01$, relative to vehicle (Vh).

DMD Fast Forward. Published on April 19, 2006 as DOI: 10.1124/dmd.105.009126
This article has not been copyedited and formatted. The final version may differ from this version.

FIG. 4. The levels of [^{3}H]MPP$^+$, HPP$^+$, and RHPP$^+$ in MDCK cells that overexpress hOCT1, hOCT2 or hOCT3. MDCK cells were transiently transfected with 1.6 μg of pcDNA3.1, pcDNA3.1-hOCT1, pcDNA3.1-hOCT2 or pcDNA3.1-hOCT3 using Lipofectamine 2000. After transfection, the cells were incubated for 24 h at 37°C. The uptake assays were usually performed after the cells formed a monolayer. **A.** The cells were incubated with 200 nM [^{3}H]MPP$^+$ for 30 min at 37°C, in the absence or presence of 50 μM phenoxybenzamine (Phe) applied to the apical cell border. **B and C.** Cells were incubated with 10 μM HPP$^+$ or RHPP$^+$ for 30 min at 37°C, in the absence or presence of 50 μM Phe applied to the apical cell border. The cellular concentrations of HPP$^+$ and RHPP$^+$ were determined by LC/MS/MS analysis. The data are presented as arithmetic mean ± SEM (n = 3). * $p < 0.05$; ** $p < 0.01$. **D.** Western blot analysis of hOCT1, hOCT2, and hOCT3 transiently overexpressed in MDCK cells. The hOCT1, hOCT2, and hOCT3 proteins have molecular sizes in the 50~75-kDa range.

FIG. 5. [^{3}H]MPP$^+$ and [^{14}C]TEA concentrations in MDCK cells that stably express the hOCT1, hOCT2, and hOCT3 proteins. Cells were incubated for 30 min at 37°C with 200 nM [^{3}H]MPP$^+$ (**A**) and [^{14}C]TEA (**B**) applied to the apical cell border. The data are represented as arithmetic mean ± SEM (n = 3). ** $p < 0.01$. (**C)** Western blot analysis of MDCK cells that stably express hOCT1, hOCT2, and hOCT3. The hOCT1, hOCT2, and hOCT3 proteins have molecular sizes in the 50~75-kDa range.

FIG. 6. Time-course analyses of HPP$^+$ and RHPP$^+$ accumulations in MDCK cells that overexpress hOCT1, hOCT2 or hOCT3. Either 10 μM HPP$^+$ (**A**) or 10 μM RHPP$^+$ (**B**)

was applied to the apical side of the monolayer of MDCK cells that overexpress hOCT1, hOCT2 or hOCT3, and the cells were incubated for 0, 5, 10, 15, 30, 60 or 90 min at 37°C. The cellular concentrations of HPP^+ and $RHPP^+$ were determined by LC/MS/MS analysis. Exponential saturation curves were fitted to the experimental data. Linear coefficient $r^2 = 0.9990$. The data are presented as arithmetic mean ± SEM ($n = 3$). ** $p < 0.01$, relative to the mock-treated cells.

FIG. 7. Concentration dependence of HPP^+ and $RHPP^+$ accumulations in MDCK cells that overexpress hOCT1, hOCT2, and hOCT3. HPP^+ was applied to the apical side of MDCK cells that stably express hOCT1 (**A**), hOCT2 (**B**) or hOCT3 (**C**), together with various concentrations of HPP^+ (0, 0.1, 0.5, 1, 2, 3, 5, 10 and 15 μM) for 15 min at 37°C. $RHPP^+$ was applied to the apical side of MDCK cells that stably express hOCT1 (**D**) or hOCT3 (**E**), together with various concentrations of $RHPP^+$ (0, 0.1, 0.5, 1, 2, 3, 5, 10 or 15 μM) for 15 min at 37°C. The cellular concentrations of HPP^+ and $RHPP^+$ were measured by LC/MS/MS. Uptake was saturatable and fitted to the Michaelis-Menten curve. Exponential saturation curves were fitted to the experimental data. Linear coefficient $r^2 = 0.9990$. The data are presented as arithmetic mean ± SEM ($n = 6$). The insert shows an Eadie-Hofstee plot of HPP^+ and $RHPP^+$ uptake, which was used to determine the kinetic parameters. *V*, velocity; *V/S*, velocity per concentration of HPP^+ or $RHPP^+$.

DMD Fast Forward. Published on April 19, 2006 as DOI: 10.1124/dmd.105.009126
This article has not been copyedited and formatted. The final version may differ from this version.

Table 1. Kinetic parameters for haloperidol pyridinium metabolites HPP^+ and $RHPP^+$ in the hOCT1, 2 and 3 stably expressed MDCK cells.

V*max* represents the maximal reaction velocity and K*m* is the substrate concentration corresponding to 50% of V*max*. The values are estimated from nonlinear least regression analysis using WinNonlin.

Compounds	Kinetic parameters	hOCT1	hOCT2	hOCT3
HPP^+	K*m* (pmol/min/μg protein)	0.99 ± 0.05	2.79 ± 0.13	2.23 ± 0.16
	V*max* (μM)	282.1 ± 4.7	256.1 ± 11.3	400.2 ± 15.2
$RHPP^+$	K*m* (pmol/min/μg protein)	5.15 ± 0.63	-	8.21 ± 0.77
	V*max* (μM)	1230.9 ± 24.8	-	1348.6 ± 36.3

Figure 1

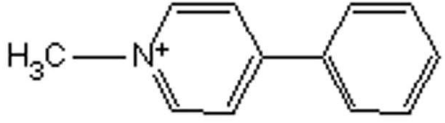

MPP+

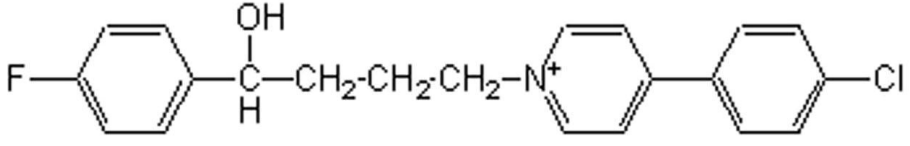

HPP+

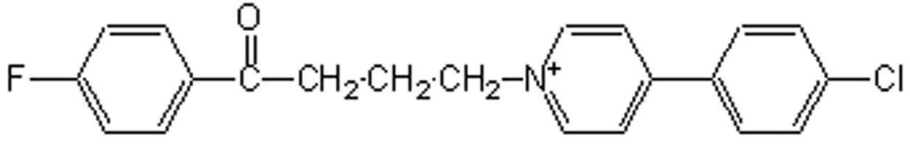

RHPP+

Figure 2

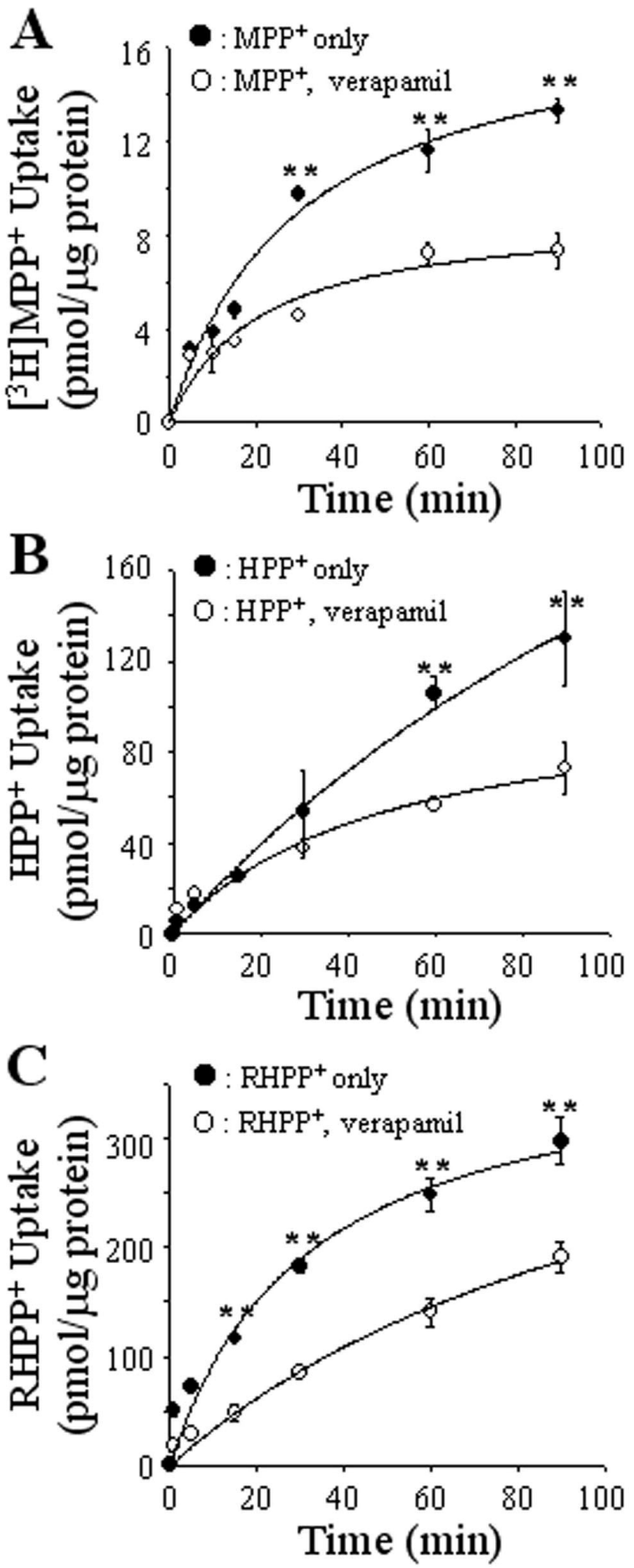
A
● : MPP+ only
○ : MPP+, verapamil
[3H]MPP+ Uptake (pmol/μg protein)
Time (min)
B
● : HPP+ only
○ : HPP+, verapamil
HPP+ Uptake (pmol/μg protein)
Time (min)
C
● : RHPP+ only
○ : RHPP+, verapamil
RHPP+ Uptake (pmol/μg protein)
Time (min)

Figure 3

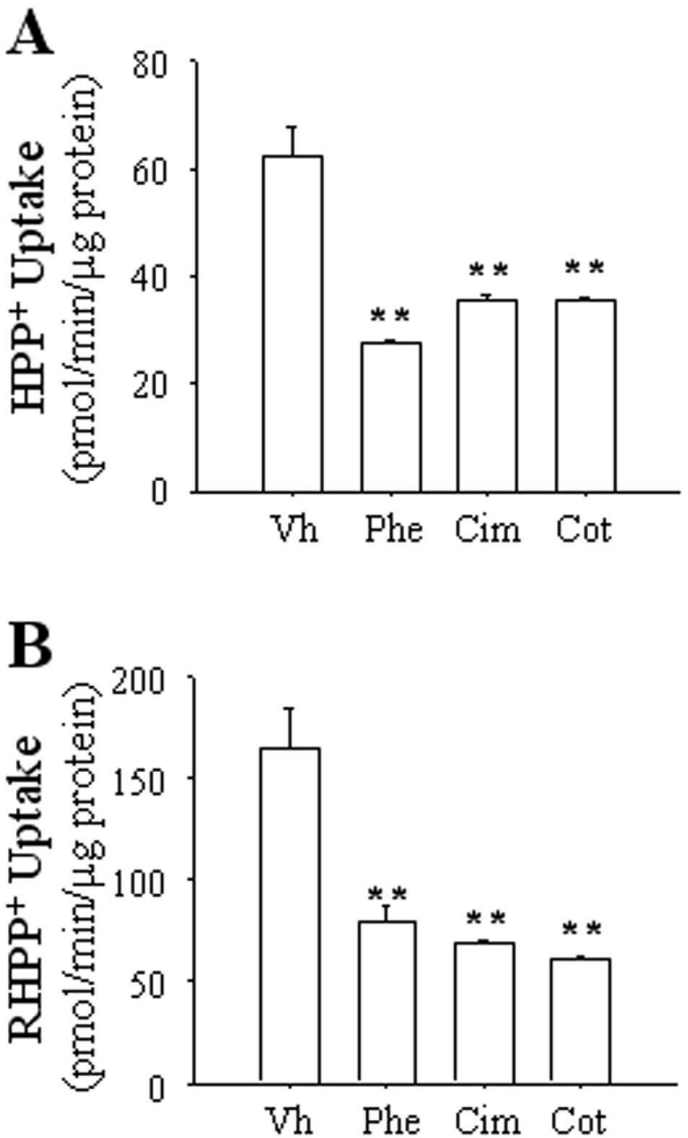
A
HPP+ Uptake
(pmol/min/µg protein)
80
60
40
20
0
**
**
**
Vh
Phe
Cim
Cot
B
RHPP+ Uptake
(pmol/min/µg protein)
200
150
100
50
0
**
**
**
Vh
Phe
Cim
Cot

Figure 4

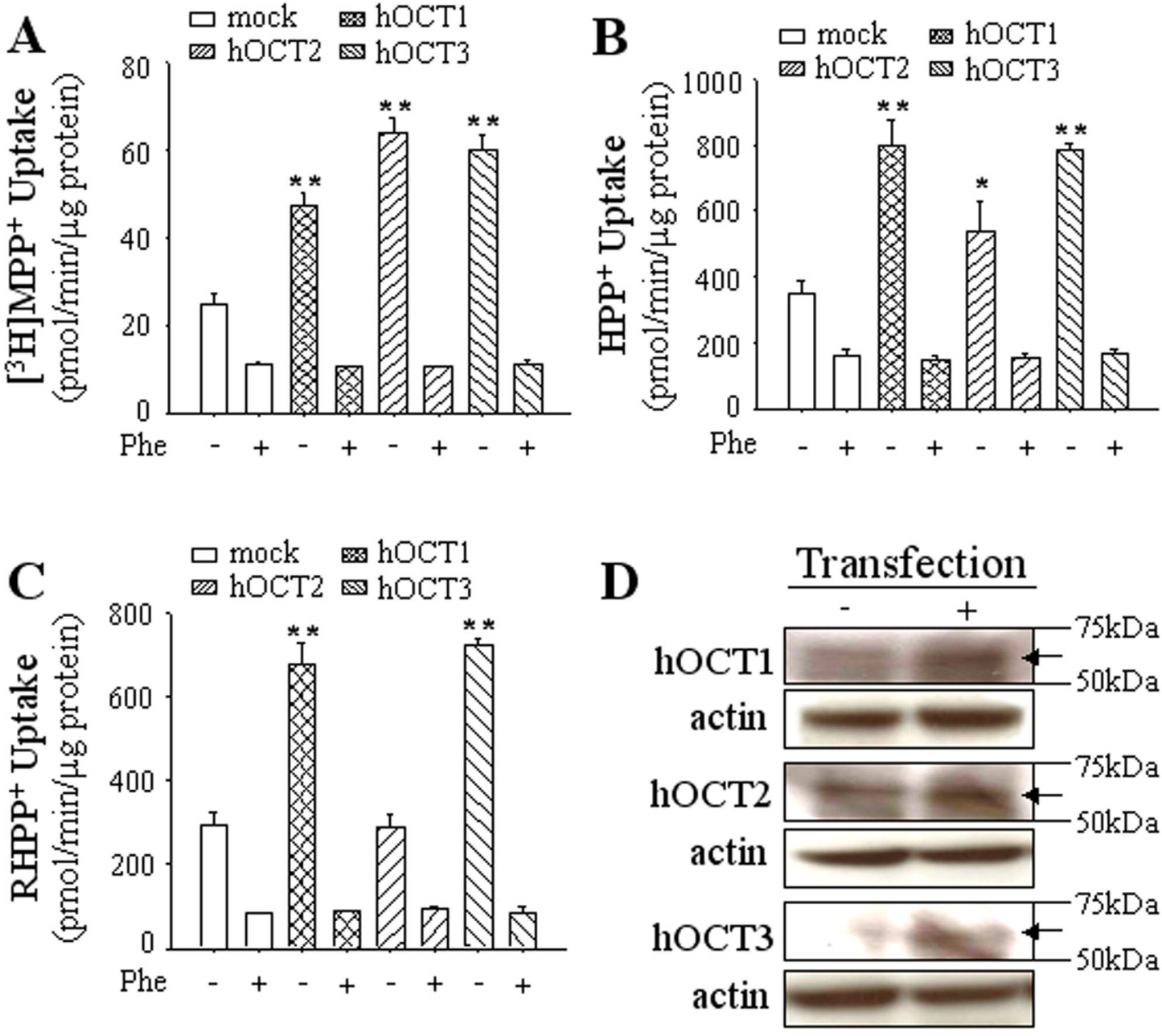
A
mock
hOCT1
hOCT2
hOCT3
[3H]MPP+ Uptake
(pmol/min/μg protein)
80
60
40
20
0
**
**
**
Phe - + - + - + - +
B
mock
hOCT1
hOCT2
hOCT3
HPP+ Uptake
(pmol/min/μg protein)
1000
800
600
400
200
0
**
*
**
Phe - + - + - + - +
C
mock
hOCT1
hOCT2
hOCT3
RHPP+ Uptake
(pmol/min/μg protein)
800
600
400
200
0
**
**
Phe - + - + - + - +
D
Transfection
- +
hOCT1
actin
hOCT2
actin
hOCT3
actin
75kDa
50kDa
75kDa
50kDa
75kDa
50kDa

Figure 5

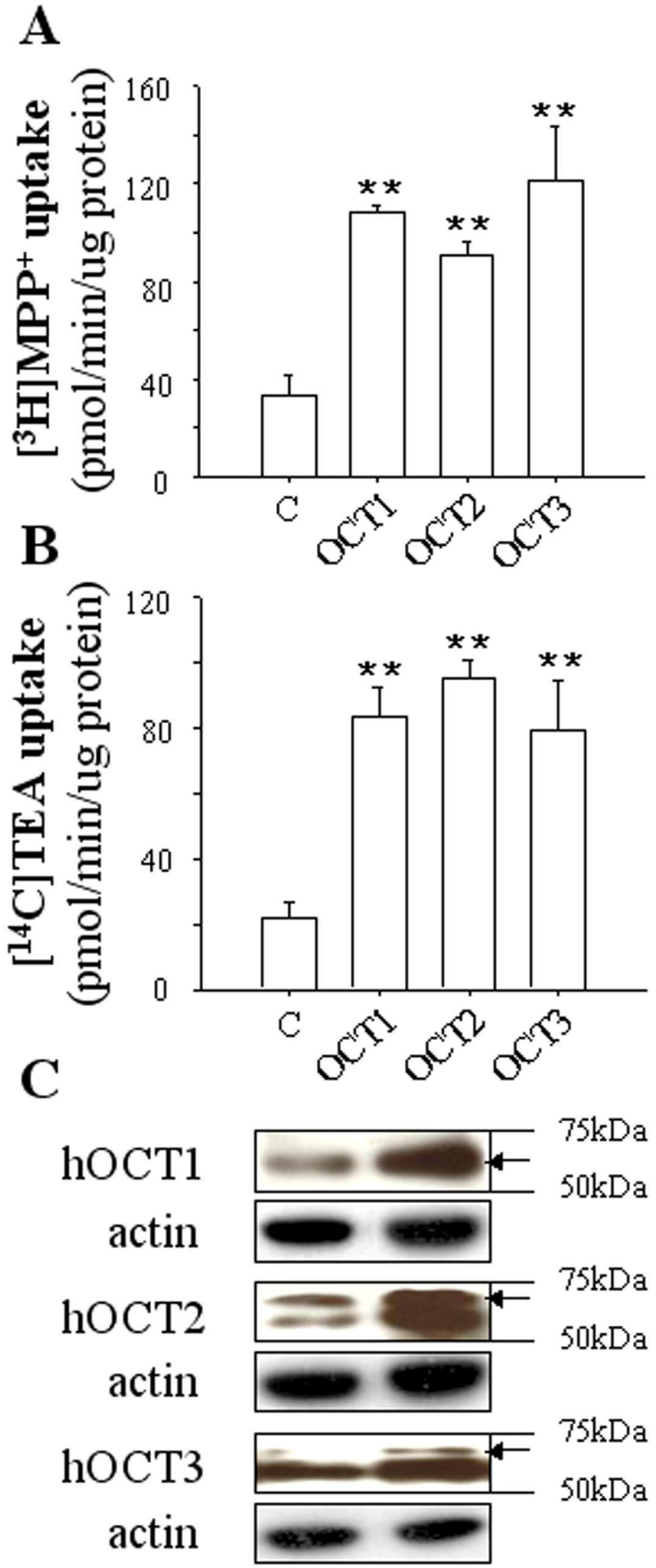
A
[3H]MPP+ uptake
(pmol/min/ug protein)
160
120
80
40
0
**
**
**
C
OCT1
OCT2
OCT3
B
[14C]TEA uptake
(pmol/min/ug protein)
120
80
40
0
**
**
**
C
OCT1
OCT2
OCT3
C
hOCT1
actin
hOCT2
actin
hOCT3
actin
75kDa
50kDa
75kDa
50kDa
75kDa
50kDa

Figure 6

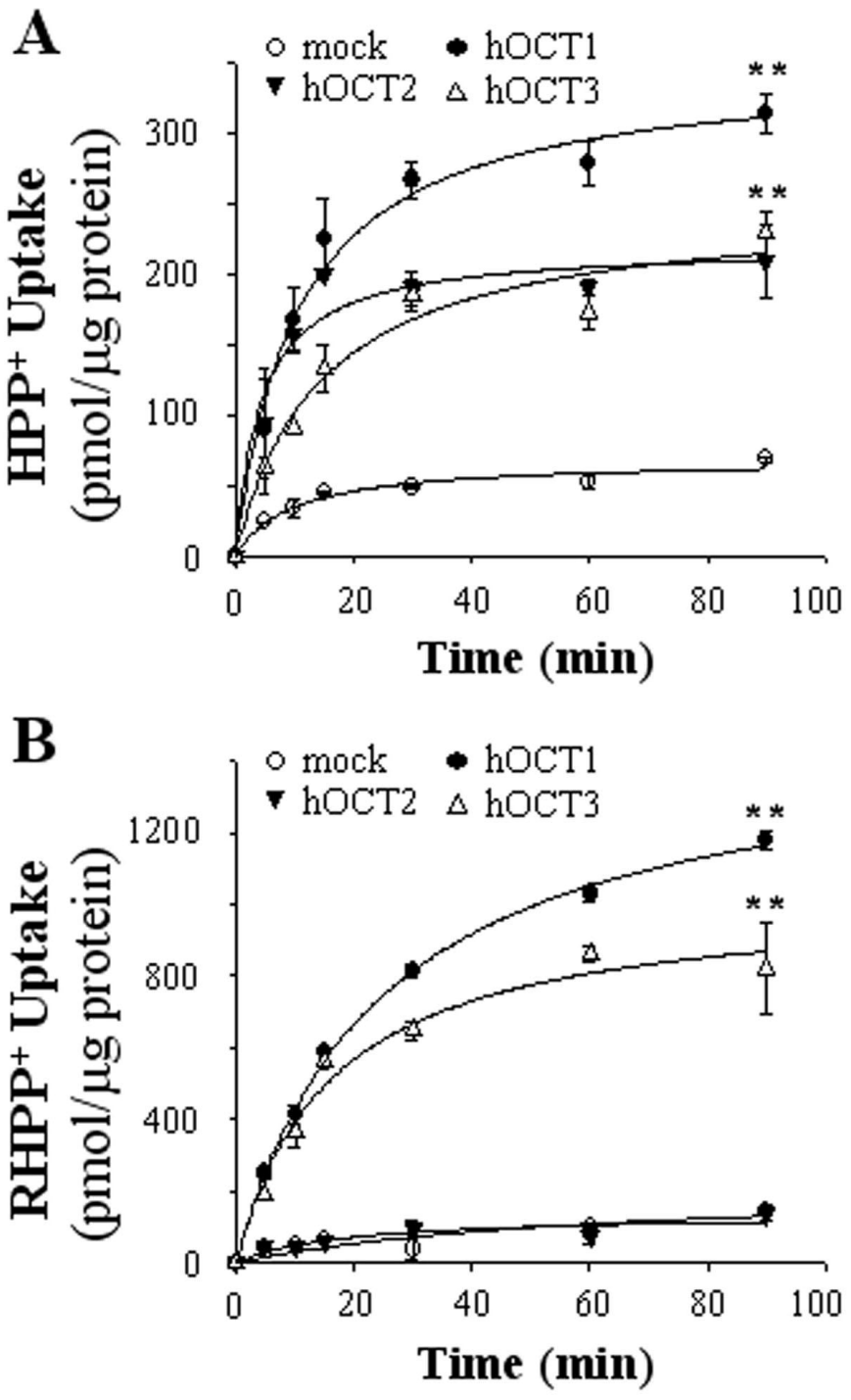
A
mock
hOCT1
hOCT2
hOCT3
HPP+ Uptake
(pmol/μg protein)
300
200
100
0
0
20
40
60
80
100
Time (min)
**
**
B
mock
hOCT1
hOCT2
hOCT3
RHPP+ Uptake
(pmol/μg protein)
1200
800
400
0
0
20
40
60
80
100
Time (min)
**
**

Figure 7

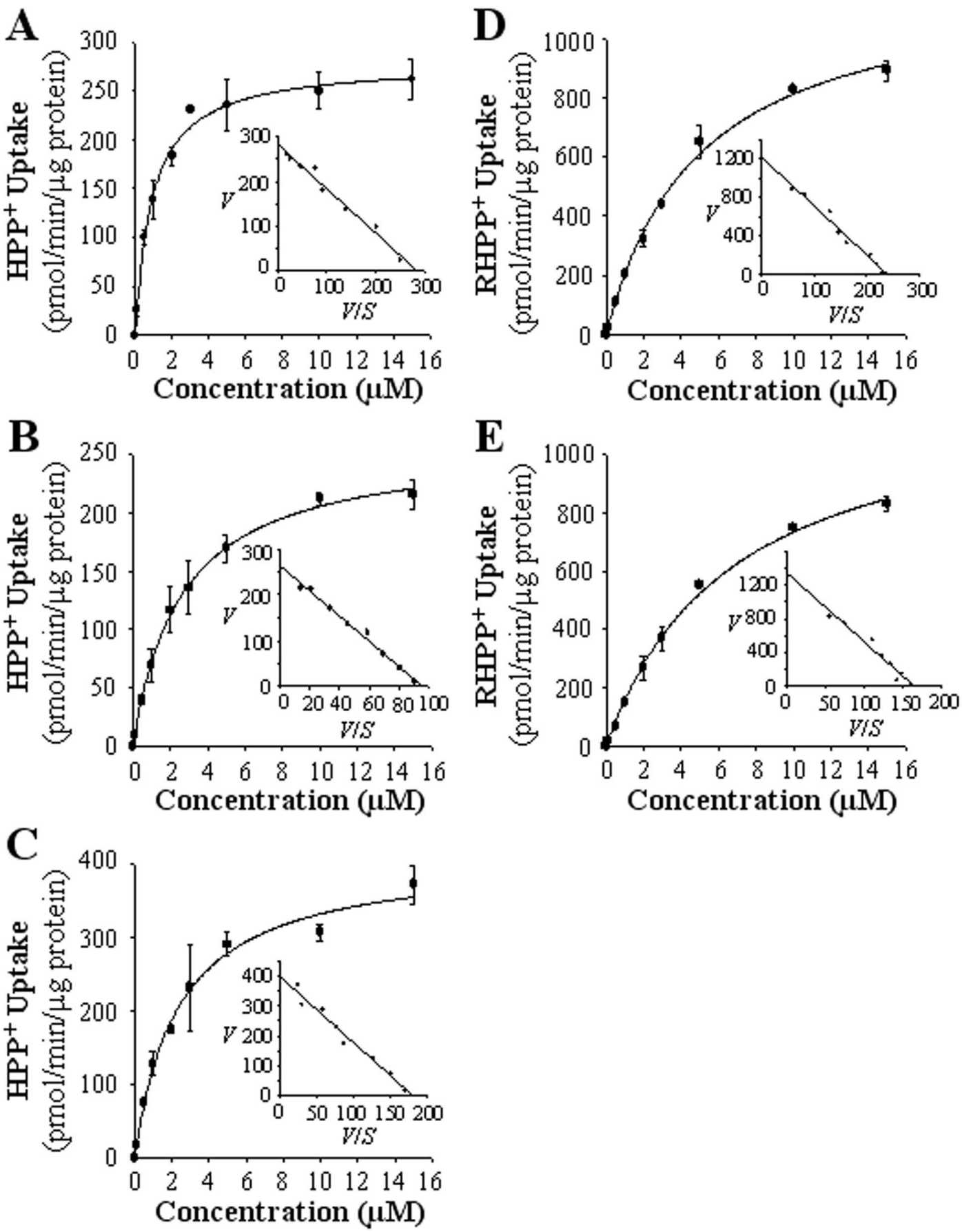
A
HPP+ Uptake (pmol/min/µg protein)
Concentration (µM)
V
V/S
B
HPP+ Uptake (pmol/min/µg protein)
Concentration (µM)
V
V/S
C
HPP+ Uptake (pmol/min/µg protein)
Concentration (µM)
V
V/S
D
RHPP+ Uptake (pmol/min/µg protein)
Concentration (µM)
V
V/S
E
RHPP+ Uptake (pmol/min/µg protein)
Concentration (µM)
V
V/S